Physica 2D (1981) 38-51

ON LANDAU AND STOCHASTIC ATTRACTOR PICTURES IN THE PROBLEM OF TRANSITION TO TURBULENCE

Victor S. L'vov, Alexey A. Predtechensky

Institute of Automation and Electrometry
Siberian Branch of Academy of Sciences
Novosibirsk
U.S.S.R.

Laminar-turbulent transition in circular Couette flow is discussed. Phenomenological equations are proposed describing the breakdown of azimuthal waves coherency. The correspondence is established between the flow turbulization and the stochastic attractor in the phase space of these equations. Evolution of attractor structure is investigated experimentally in terms of motion in some effective phase space. It is shown that during the transition to turbulence the increase in number of degrees of freedom is combined with the stochastic behaviour of rapid motion envelopes.

INTRODUCTION

Today the idea that a hydrodynamic turbulence of viscous fluid can be described by finite set of ordinary differential equations has received general recognition. The actual questions are the number and the type of equations one should take into account for a concrete flow at given Reynolds number to be described with reasonable accuracy. For the reduction of input equations, the method of approximating functions (e.g.Galerkin method) is often used. However, generally speaking, an arbitrary basis will not be an eigenbasis even for the simplest motions arising beyond the onset of instability. It leads to unreasonably great number of governing equations. For example, 12 equations were used for description of thermal convection in Hele-Shaw cell [1]. Later on it was found (see, e.g., [2]) that only four degrees of freedom are effectively exited at a first stage of turbulization, so for description of the experiment it is sufficient to solve eight equations. Further, 39 equations of Galerkin approach to thermal convection were required for a qualitative description of the transition to stochastic flow in the layer heated from below [3]. For more complex flows the number of such equations appear to be still greater. Moreover, a truncation of formal Galerkin sets can lead to alteration in subtle topological characteristics of the original many-dimensional attractor - a stochastic attractor can be transformed into an intricate limiting cycle (closed orbit). Further truncation of the model can transmute this cycle into a new stochastic attractor again. The well-known Lorenz system [4] is apparently an example of such reduction. Therefore it remains unclear if attractors constructed in this way have a real concern with the problem of fluid turbulization.

Meanwhile there is quite a number of flows at transitional Re numbers when most of the flow energy is concentrated in narrow frequency bends of power spectrum so that a velocity $V(r,t)$ may take a form

$$V(r,t) = 1/2 \sum (A_j(r,t)\exp(i\omega_j t) + c.c) \qquad (1)$$

In some small Re-region the spatial structure of the modes ω_j has a negligible alteration so it can take the form $A_j(r,t) = A_j(t)\cdot f_j(r)$. (In the cases of high symmetry of flow there can exist a degeneration - some various spatial motions can

be centered at the same frequency). Since a characteristic variation time of A(t) is sufficiently less than revers distance between frequencies ω_j, it is possible to construct phenomenological equations for temporal envelopes $A_j(t)$

$$dA_j/dt = \gamma_j A_j + \sum_k (\eta_{kj} + iT_{kj}) |A_k|^2 A_j + \ldots , \qquad (2)$$

taking into account only the resonant terms. The envelope representation (2) can be formally obtained by Galerkin approximation of input equations through averaging in a fibre over the many-dimensional non-resonant torus of rapid motions and further reduction to Poincare normal form in the vicinity of singular point (see [5]). In this way the coefficients in (2) and the spatial structure of motion $f_j(r)$ can be obtained in principle.

It is essential that the number of non-trivial equations in (2) (i.e. the number of effective degrees of freedom) can be less than the dimensionality of initial model because this number is determined by the number of the most intensive peaks observed in the power spectrum (in the absence of degeneracy). For example, only one equation of type (2) should be investigated to understand the pecularities of the secondary flow arising. This approach gives the Landau law [6] $|A|^2 \sim \alpha(Re - Re_c)$ which is well fulfilled in experiment. The Navier-Stokes equations are required only for calculation of two coefficients α and Re_c.

It seems reasonable to use this phenomenological approach also for investigation of next bifurcations in flows with soft, stepwise transition to turbulence. Hence it becomes clear that there is a strong lack of experimental information in this field. Also a new language for description of experimental data appears. This language can also be used for a number of questions to be formulated to an experimentator. These questions are: how can the number of necessary equations be determined proceeding from the results of experiment, or what is the dimensionality of effective phase space? How can the character of motion be determined in this phase space, or, in other words, what does an experimental attractor look like? How does its structure change as Re grows? And finally, what is the correlation between the attractor structure observed in the experiment and the structure numerically obtained from the phenomenological model?

Here we shall discuss these questions taking as an example the laminar-turbulent transition in circular Couette flow with the inner cylinder rotating. The hydrodynamic cell was formed by two concentric stainless steel cylinders (d_i = 35mm, d_o = 55mm, h = 302mm) with radial throbbing less than 5 μm. The water temperature was maintained to an accuracy of 0.02°C. The stability of rotation period was controlled to an accuracy of 10^{-4} per revolution and the long-time stability was defined by quartz generator. The azimuthal velocity component $V_\varphi(t)$ was measured by Laser-Doppler velocimeter [7] for the flow to be non-perturbed. Up to 256 thousand samples $V_\varphi(n\tau)$ with nessesary sampling time τ were analized using the computer system for data acquisition and processing [8] .

We shall discuss two variants of fluid behaviour evolution discriminated by initial numbers of Taylor vortices. Comparing these results with those [9,10] obtained in other cells we come to the conviction that a number of basic qualitative characteristics of the transition is quite common despite of some discrepancy in concrete details. Therefore it should be expected that the Couette flow with the inner cylinder rotating is a suitable model for investigation of common features of soft, stepwise transition to turbulence.

1. POWER SPECTRA EVOLUTION

In accordance with the above, at the first step of investigation the number of rapid motions and the order of their rise should be determined. This information is given by the evolution of the power spectra $J(\omega)$. For the case of sharp component presence, the power spectrum must be calculated in the direct way:

$$J(\omega) = \langle |V_\omega|^2 \rangle = 1/M \sum_{p=1}^{M} |V_p(\omega)|^2$$

where $V_p(\omega)$ is the discrete Fourier transform of the block of initial discrete velocity data, M is the total number of these blocks.

The Taylor vortices arise in the cell discussed at Re = $\omega_m(d_o - d_i)d_i/4\nu = 74^{+}_{-}2$, where ω_m is the rotation frequency of inner cylinder and ν is the kinematic viscosity. In this cell one can obtain several supercritical stable spatial states

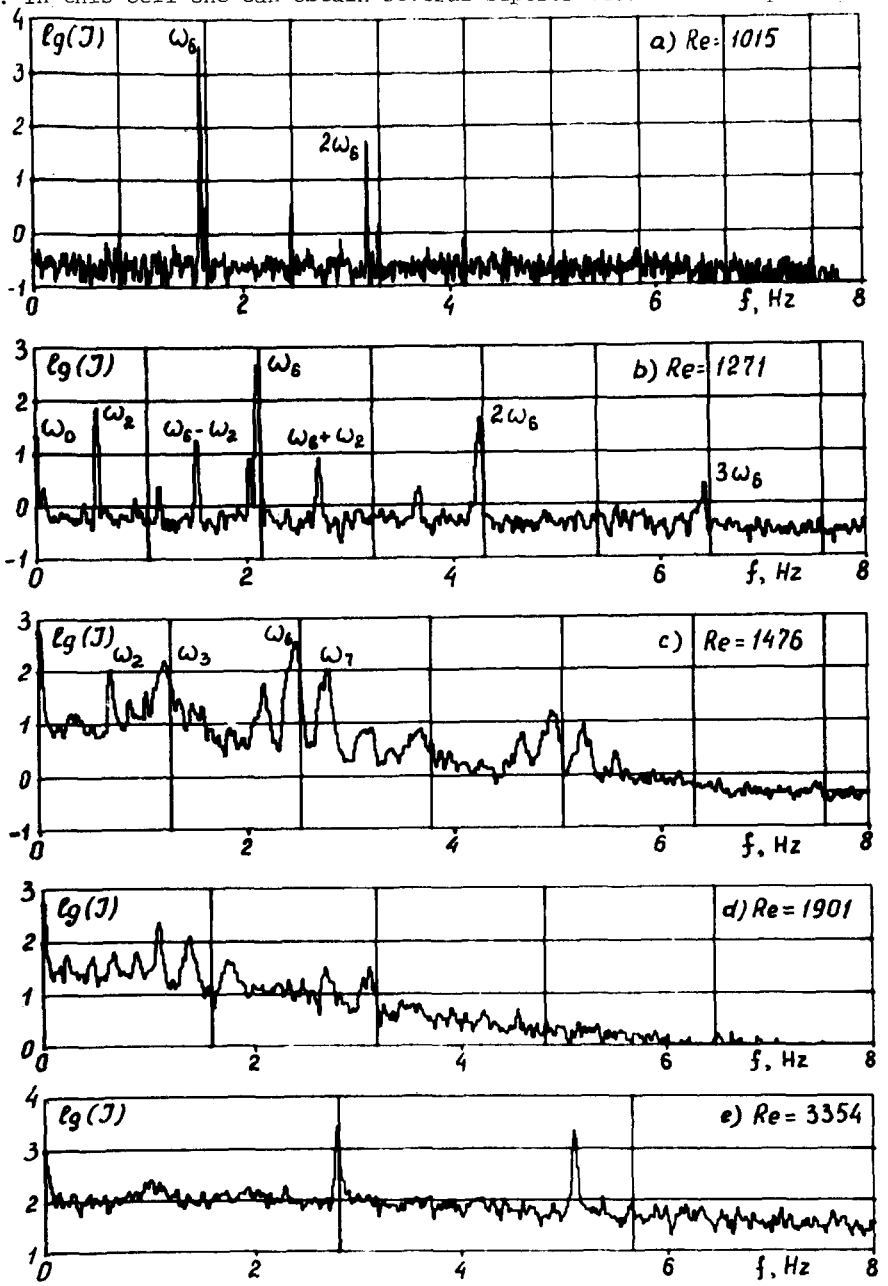

Figure 1. The velocity fluctuation power spectra for N=30. Vertical lines give the scale in units of inner cylinder rotation frequency The Hanning window was used giving the frequency resolution ~8·3/512 Hz.

characterized by different numbers of vortices varying from 22 to 36. We shall discuss the results corresponding to the states with N=30 and 28 and obtained under a slow adiabatic acceleration of the inner cylinder.

1.1. SPECTRUM EVOLUTION FOR N=30

In this state the bifurcation - the bends of Taylor vortices, or azimuthal waves - - takes place at Re-region from 995 to 1015. It is detected by the appearance of a narrow peak at the frequency $\omega_6 = 1.93\omega_m$ in the power spectrum - see Fig.1. In accordance, with previous observations [7] we assume this mode corresponding to six bends over the circumference orbit. The critical number Re_1 can be determined to an accuracy of ± 1 in each run. The cause of Re being different from run to run is discussed in Section 2.

The ω_6-peak magnitude obeys the Landau Law $I_6 \sim Re - Re_1$ in the region of small supercriticalities $\varepsilon = \Delta Re/Re_1 < 0.02$ (see Fig.2) where the relative linewidth is less than $1.2 \cdot 10^{-3}$ at the level 10^{-3}. At ε greater than 0.02 a series of fine bifurcations takes place resulting in some broadening of the spectral line. Simultaneously a low-frequency motion ω_o appears. These phenomena will be discussed in detail in the next Section.

With a further increase in Reynolds number the second independent peak at the frequency $\omega_2 = 0.55\omega_m$ appears in the power spectrum and after that the combinative frequencies $\omega_6 \pm \omega_2$ become significant (see Fig.1b). At $\varepsilon > 0.25$ the next peak appears at the frequency $\omega_3 = 0.95\omega_m$. Further the peak widths gradually become comparable with the distanses between them. This is illustrated in Fig.3, where the dependences of the frequencies ω_2, ω_6 and of their widths on Re number are shown. At Re = 1600 already no pronounced maxima are observed in the power spectrum - see Fig.1d. At still greater Re numbers the system of reemerged peaks like in [10] is observed. For instance, at Re = 3350 (Fig.1e) two relatively narrow peaks at the frequencies $\sim\omega_m$ and $1.81\omega_m$ are distinctly observed. This system of secondary peaks is destroyed at Re $\sim$ 12000.

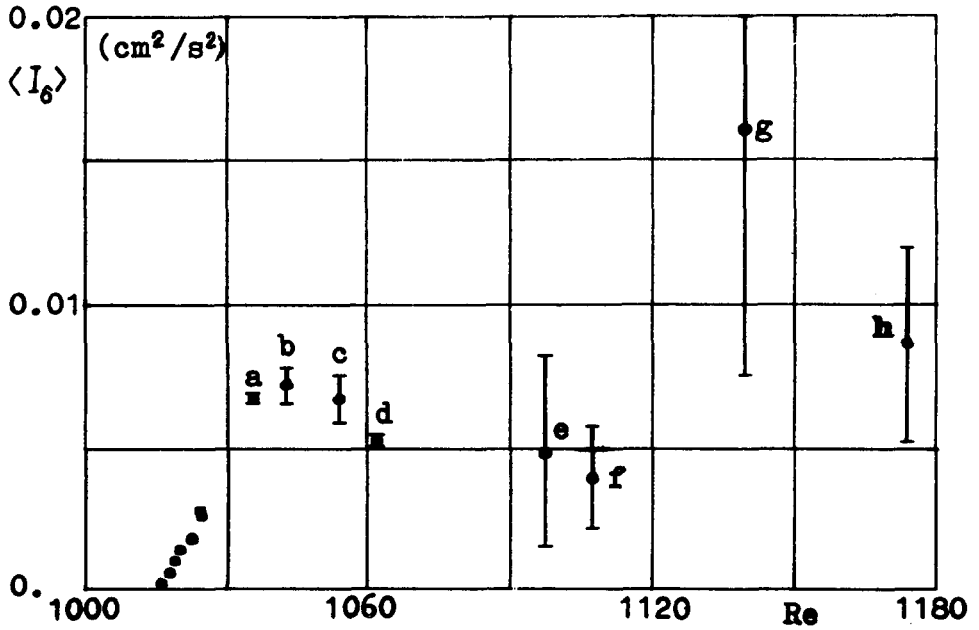

Figure 2. Mean amplitude of ω_6-motion and its dispersion (vertical bars) vs. Reynolds number.

Figure 3. The centre frequency and linewidth (full-width at the level 0.1) of peaks ω_6 and ω_2 vs. Re number for N=30.

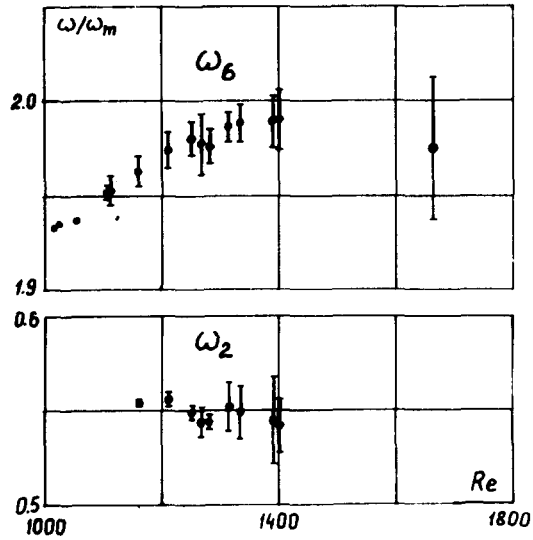

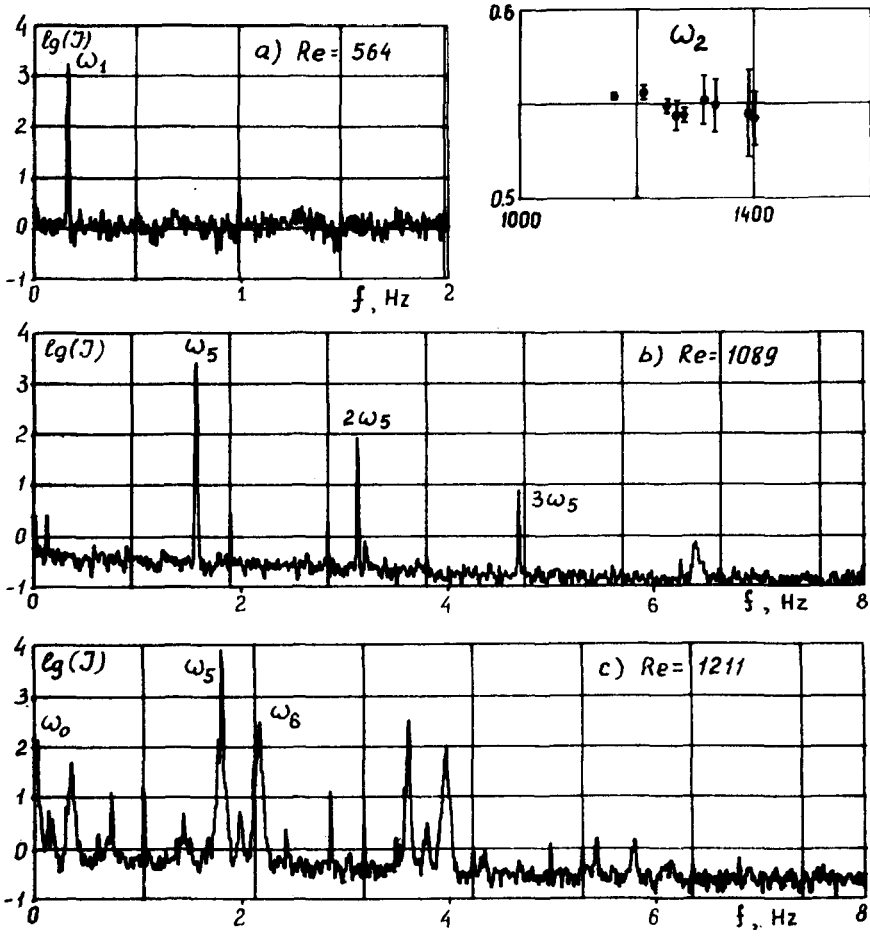

Figure 4. Power spectra evolution for flow state with N=28

1.2. SPECTRUM EVOLUTION FOR N=28

The system of 28 Taylor vortices loses its stability significantly earlier then the system of 30 vortices. At Re = 564 (see Fig.4a) a single narrow peak at the frequency $\omega_1 = 0.33\omega_m$ is observed, which situation remains until Re = 900. In the Re region from 900 to 980 the peak ω_1 dissappears and a peak at the frequency

Table 1. Bifurcational values of parameters for the first rearrangements of Couette flow

Reference	[11]		[9]
Height/gap	30		20
gap/inner radius	0.57		0.14
Taylor vortices appearance at Re_c =	74 ± 2		120
Number of vortices N	30	28	17
First azimuthal wave appearance at Re_1/Re_c	13	6,5	1.3
Number of waves over the circumference orbit	6	1	5
Stability region of the first azimuthal wave $(Re_1' - Re_1)/Re_1$	0.025	0.8	4.4

$\omega_5 = 1.63\omega_m$ appears - see Fig.4b. Next bifurcation leads to appearance of fine structure of the ω_5-peak as in the case of ω_6 peak and N=30. It is clear that there arises the ω_0-motion.

In the Re region from 1100 to 1200 a full rearrangement of spatial state occurs - the system of vortices transforms to the state with N=29, and a series of new broaden peaks appears (see Fig.4c). We remark that the state N=29 may arise from the very beginning. This third way to turbulence was described in [11] . Here we shall indicate only that at $Re > 1400$ the difference between evolutions for N=29 and N=30 gradually disappears.

Thus, there are several ways to turbulence in the cell discussed. In other cells with narrow gap other "ways" were observed [9,10] . All these "ways" differ in concrete magnitudes of bifurcational Reynolds numbers and types of motions - see Table 1.

Dispite of this discrepancy the rearrangements of a flow in these cells have a number of similar features. Namely, the next bifurcation (after the Taylor one) developes into azimuthal waves of any wavelength in both narrow and wide cell. In both cases one can observerd both the appearance and further disappearance of a narrow peak as Re is increased. In both cases [8,10] there is a reemergent order on the background of developed turbulent motion. This coupling of variety and similarity of the transitional flow characteristics gives hope that the detailed study of circular Couette flow will be quite useful for the complexity of laminar-turbulent transition to understand.

2. BREAKDOWN OF AZIMUTHAL WAVES COHERENCY

We shall discussed here the behaviour of the ω_6-motion at N=30, when the ω_6-peak in the power spectrum begins to broaden. We shall show that this phenomenon is determinant and connected with the onset of fluid motion stochasticity.

2.1. EXPERIMENTAL RESULTS

First of all it is natural to consider the peak evolution with higher frequency

and Reynolds nimber resolution - see Fig. 5. It is seen that the spectral line possesses a complicated fine structure which is various at various Re, and it is difficult to say anything more certain. What should be much more informative, as stated above in the Intoduction, is the temporal dependence of ω_6 -motion envelope. It may be considered as a projection of phase trajectory of the system onto some axis of effective phase space. This dependence can be computed from velocity data, for example, by following direct algorithm:

$$I_6(t) = |A_6(t)|^2 = \quad (3)$$
$$= \left|\Omega/(2\pi)^{1/2}\int_{-T}^{T} V_\varphi(t-\tau)\exp(i\omega_6(t-\tau) - 1/2\,\Omega^2\tau^2)\,d\tau\right|^2.$$

In Fig.6. is shown a set of such dependencies. These results are obtained from the run where Re $= 1015 \pm 1$. Such behaviour is characteristic and repeats in each run to an accuracy of some details. The amplitudes of mean intensity and its dispersions corresponding to this run are shown in Fig.2. The first regime (Figs.5a and 6a, Re = 1035) at supercriticality $\varepsilon < 0.02$ corresponds to the stable periodic motion at the frequency ω_6. The image of this motion in the input phase space is a simple limiting cycle, or a closed orbit, corresponding to a fixed point of the averaged system. In general it is not quite obvious because there also exists a significant motion at the frequency $2\omega_6$. But below we shall show that this motion is fully determined by the ω_6-motion. Some finite value of noise on the straight line $I_6 = \text{const}$ is connected, by all probability, with the noise of the velocimeter.

The next two regimes (Figs.5c,6b,6c) correspond to Re = = 1043 and Re = 1054 wich exeed some bifurcational value Re_1^1. Above this value a slow sinusoidal modulation of the basic motion ω_6 arises with a frequency ω_o which grows as ε increases. This modulation is distinctly seen in Fig. 6c but cannot appear in the correspondent spectrum due to the limit of record time in this regime.

Below the Reynolds number discussed the flow develops in agreement with the Landau hypothesis - the three consequent bifurcations $Re_c = 74$, $Re_1 = 1015$, $Re_1^1 = 1040$ result in consequent addition of degrees of freedom characterized by spatial and temporal periodicity. It may seem that the stationary state of fluid motion in this case can be represented by a phase point moving along the surface of a stable three-dimensional torus. But is not quite correct because the Taylor virtex periodicity is deformed by edges of an experimental cell and, hence, is not a real space-homogeneous periodicity. Therefore it would be more correct to speak about the motion on the two-dimensional torus.

At a further increase in Re number there exists a series of neighbouring states but observation of these motions is hampered by extraordinary slowness of transition to the

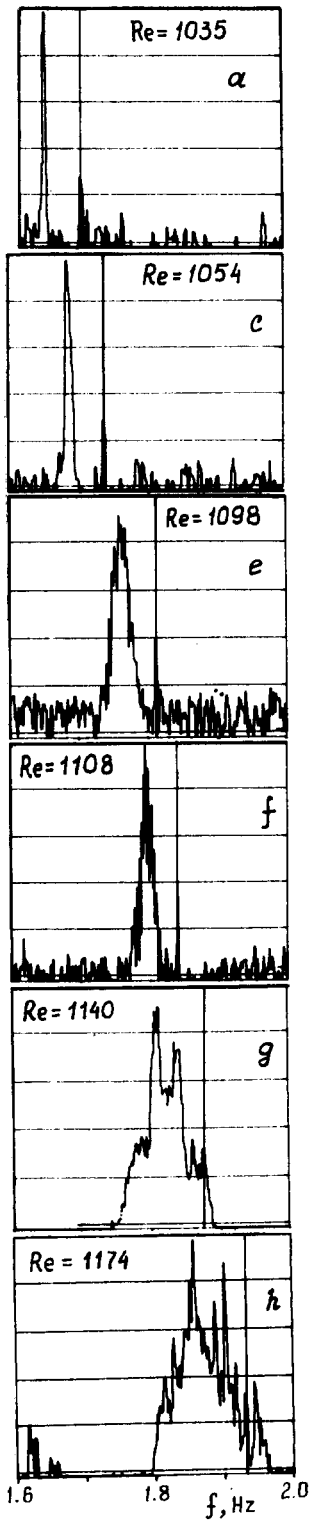

Figure 5. Fine structure evolution of ω_6-peak. N=30, vertical line indicates the frequency $2\omega_m$

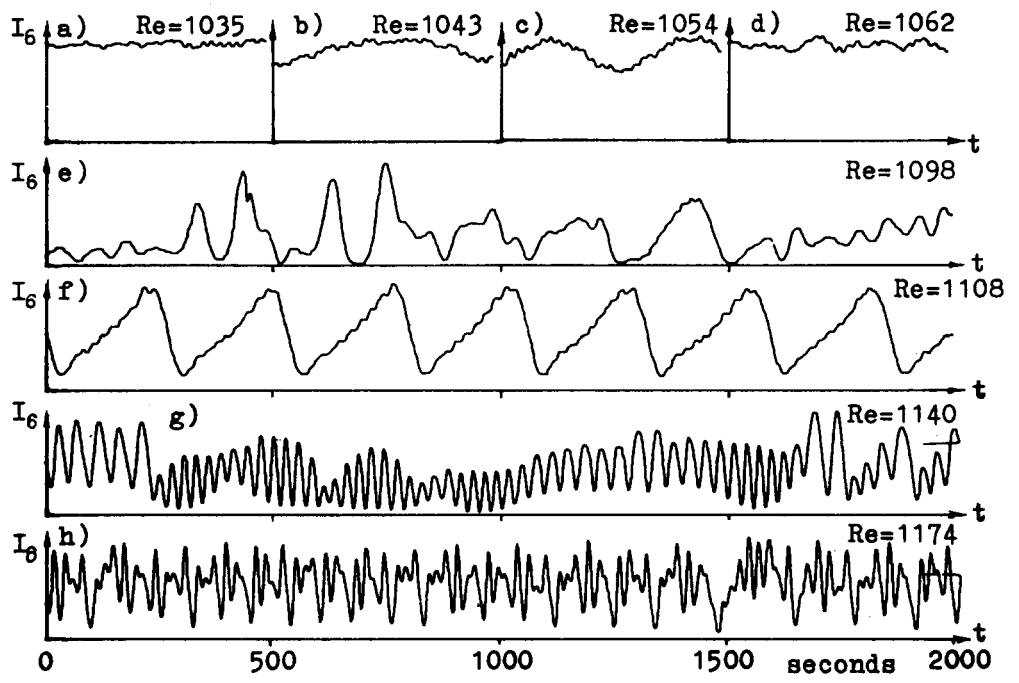

Figure 6. Temporal dependences of ω_6-motion envelope. Frequency window is $\omega_6(1 \pm 0.02)$.

steady state. Therefore there is no full confidence that the states described below immediatly follow one another. Thus, at Re = 1062 the modulation described above disappears - see Fig.6d. At Re = 1098 the complicated modulation develops which can be called chaotic as far as it can be concluded from the observation during 2000 seconds. The ω_6-peak in this state (see Fig.5e) is found to be noticeably broadened. It is very interesting that with growing Re the chaotic modulation transforms into a periodic one again, this time not sinusoidal but sawtoothed - see Fig.6f. Further at Re = 1140 the character of modulation becomes complicated again. Possessing some imagination one can see the alternated fragments of sinusoids with two different frequencies. This can be easy seen in Fig.5g from the spectrum consisting of two distinct broad peaks. It should be noted that in this case the modulation frequency is significantly higher than that in the previous regime. At Re = 1174 on the right slope of the spectral peak one can see a narrow line with two satellites that indicates the presence of periodical component which was not observed in the preceding regime.

At greater Reynolds numbers the ω_2 - motion appears. We shall discuss this phenemenon in Section 3.

2.2. PHENOMENOLOGICAL MODEL

Now we consider the regimes at small supercriticalities above the Re_1 - threshold. There are only two significant motions - ω_6 and $2\omega_6$. In accordance with this fact the system (2) takes the form:

$$dA/dt = \gamma A + V_1 BA^* + W|A|^2 A, \tag{4a}$$

$$dB/dt = -\tilde{\gamma} B + V_2 A^2. \tag{4b}$$

Since $\gamma(Re) = 0$ at $Re = Re_1$, it is reasonable to set $\gamma = \alpha(Re - Re_1)$. At small supercriticalities $\gamma \ll \tilde{\gamma}$ and therefore the characteristic time of motion should be

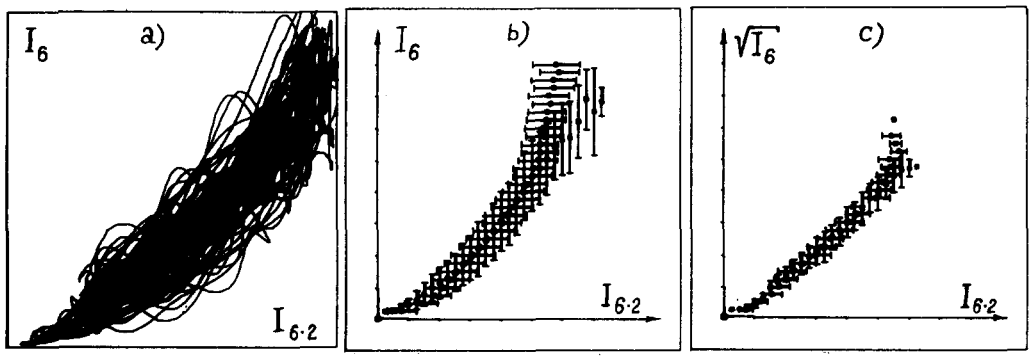

Figure 7. a) Projection of phase point trajectory onto the plane I_6 - $I_{6\cdot2}$; b) Superposition of regression lines: $\langle I_6 \rangle$ vs. $I_{6\cdot2}$ and $\langle I_{6\cdot2} \rangle$ vs. I_6 ; c) The same picture but $I_{6\cdot2}$ is replaced by $\sqrt{I_{6\cdot2}}$.

much greater than $1/\tilde{\gamma}$. It means that $dB/dt \ll B\tilde{\gamma}$ and B is the forced motion:

$$B = V_2 A^2 / \tilde{\gamma} \qquad (5)$$

The domain of Re numbers where this relation is valid can be found experimentally. Firstly, it follows from (5) that the phases of A - and B - motions must be rigidly correlated: $2\psi_A - \psi_B = \text{const}$, and therefore the module of correlator

$$|K(\omega_6, 2\omega_6)| = |\langle V(\omega_6) V^*(2\omega_6) / |V(\omega_6) V(2\omega_6)| \rangle|$$

must be equal to unity. This value computed from experimental data remains equal to 0.98 0.99 up to Re 1300, i.e. up to the Re numbers that are much greater than those discussed. Secondly, the variables $I_6 = |A_6(t)|^6$ and $I_{6\cdot2} = |B(t)|^2$ computed from the velocity data by (3) can be considered to be a parametrical representation of phase trajectory projection onto some X - Y plane - see Fig.7a. Since this trajectory has a noisy component, it is reasonable to construct a probability density of sojourn of the system in various points of such plane and further to analyse the lines of regression - $\langle X \rangle$ vs. Y and $\langle Y \rangle$ vs. X. The results of such processing are shown in Fig.7b, where the vertical and horizontal bars indicate the corresponding dispersions. It can be concluded from Fig.7b that the regression lines are disposed along a parabolic curve corresponding to the collorary from (5): $|B(t)| \sim |A(t)|^2$. This fact is traced more distinctly if B(t) is replaced by $\sqrt{B(t)}$ - see Fig.7c, where the parabola transforms into a straight line. All this means that the motion at the frequency $2\omega_6$ is a forced motion and therefore the system (4) takes the form:

$$dA/dt = \gamma A + (iT - \eta) |A|^2 A, \qquad (6)$$
$$\gamma = \alpha(Re - Re_1).$$

This equation possesses an unique solution presenting the Landau law: $|A|^2 = \gamma/\eta = \alpha(Re - Re_1)/\eta$. For our case this law is well fulfilled up to $\varepsilon = 0.02$ when the stable clozed orbit exists, as it can be seen from Fig.2.

Due to the absence of non-stationary solutions at $t \to \infty$, the equation (6) cannot explain the appearance of temporal dependence of A. The thing is that when deriving eq. (6) we supposed the absence of degeneracy, considering the - flow to be described by unique spatial function. Meanwhile the visual observations show that the boundary between a pair of vortices is almost immovable even if the amplitude of bends is rather big. It means that under first approximation the flow in each pair is independent of the motions of other pairs and for the bends amplitude of each vortex pair numbered n its own equation of type (6) must be written - see the first line in (7). Thus the ω_6 - motion possesses a high multiplicity of degeneration connected with the high height/gap ratio: $h \gg (r_o - r_i)$. For the construction of rough phenomenological model to be finished, we take into account the interaction between the neigbouring vortex pairs but only in linear approximation due to the fact that this interaction is small compared to the "internal interaction" in pairs:

$$dA(n)/dt = \gamma A(n) + (iT-\eta)|A(n)|^2 A(n) - 1/4(a+ib)(2A(n) - A(n+1) - A(n-1)). \qquad (7)$$

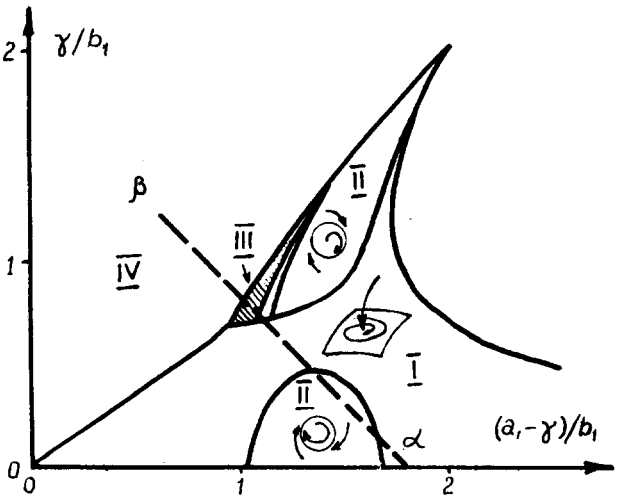

Figure 8. Domains of different behaviour of solution for eqs.(12) (according to [13]). If Re is increased, γ grows and system moves along α - β .

Here it should be supposed that $\gamma > 0$, $\eta > 0$. Without loss of generality we may assume that $a > 0$. Since these equations have to be investigated in a small domain of Re numbers, it is possible to suppose that only γ is Re-dependent but the other coefficients are some constants.

Equations (7) posses a space-homogeneous solution

$$A(n) = A\exp(i\gamma tT/\eta), \quad |A|^2 = \gamma/\eta , \tag{8}$$

coinciding with the solution of eq.(6). Besides there is a set of more complicated solutions in which the slow amplitudes of azimuthal waves in adjacent vortex pairs have some phase shift 2ψ : $A(n) = A\exp(2i\psi n)$. For the simplicity of consideration we shall assume that there are no zero boundary conditions for the azimuthal waves at the edges of cell but the phase shift takes on values from a discrete set $\psi_m = 2\pi m/N$, where $M = 1,2,\ldots, N/2$ and N is the total number of vortices. The critical Reynolds number $\widetilde{Re}_1$ corresponding to appearance of this solutions is greater than Re_1 : $\alpha(\widetilde{Re}_1 - Re_1) = a\cdot\sin^2\psi_m$. Perhaps, it is this fact that can explain the difference in critical values Re_1 observed in different runs.

To investigate the stability of the simplest solution (8) with respect to amplitude modulation we assume:

$$A(n) = A\exp(i\gamma tT/\eta)(1 + \delta A\cdot\exp(\nu_m t + 2i\psi_m t))$$

By linearizing the egs.(7) with respect to δ we obtain the instability increment:

$$\nu_m = -(\gamma + a_m) + (\gamma^2 - b_m(b_m - 2\gamma T/\eta))^{1/2}$$
$$a_m = a\cdot\sin^2(\psi_m), \quad b_m = b\cdot\sin^2(\psi_m).$$

If $bT < 0$ then $\nu_m < 0$ and the solution (8) is stable. This case seems to be realized in the experiments [9,10] with a narrow gap, as well as in our cell for the - mode in the state N = 28. If $bT > 0$ and $bT > a\eta$ then the space-homogeneous solution (8) is instable with respect to the modulation disturbances numbered $m = 1,2,\ldots,$ which obey the inequality

$$\sin^2(2\pi m/N) < 2\gamma/\eta\,(bT - a\eta)/(a^2 + b^2). \tag{9}$$

At small supercriticalities above the Re_1 - threshold (at small γ) not a single positive m obeys this inequality and thus the solution (8) is stable. The instability threshold Re_1' is obtained from (9) at m = 1:

$$\alpha(Re_1' - Re_1) = (a^2 + b^2)\sin^2(2\pi/N)/(bT - a\eta). \tag{10}$$

Within Re - domain

$$Re_1' - Re_1 < Re - Re_1 < 4(Re_1' - Re_1) \tag{11}$$

only a single disturbance m = 1 is unstable. Hence only this disturbance will be quite essential in the Re-domain (11). By neglecting the rest of the disturbance types we obtain from (9):

$$dA/dt = \gamma A + (iT-\eta)((|A|^2 + 4|A_1|^2)A + 2A_1^2A^*)$$
$$dA_1/dt = (\gamma-a_1-ib_1)A_1 + (iT-\eta)((2|A|^2 + 3|A_1|^2)A + A^2A_1^*). \quad (12)$$

Here the dimensionality of effective phase space is reduced from N - 1 to 3.

Under some redenotations the equations (12) coincide with equations investigated by Rabinovich and Fabricant [13] under the following limitations of parameters: $\eta = 0$, $\nu = -\gamma + a_1 > 0$. The plane of parameters of eqs. (12) is shown in Fig.8 where the domains of different behaviour of solutions are marked according to [13]. In particular, if a and b in (7) obey the inequality $b < a < 2b$ and Re increases, then the system will move along the $\alpha - \beta$ line crossing successively the following domains: I - the domain of stable equillibrium - A = const, A_1 - const; II - the domain of periodic variation of A and A_1 ; III - the domain of complicated and stochastic behaviour and IV - the domain of bounded solution absence if $\eta = 0$. If $\eta \neq 0$ then a new fixed point exists.

It should be noted that at $\eta = 0$ the limitation of rapid oscillations occur due to the leakage of energy into a modulational motion only. But the existance of the Landau law in our case shows that the non-vanishing value of η is of principal significance. Despite of this fact it is very interesting that the same sequence of regimes is observed in the experiment discussed at Re increasing from 1040 to 1100. The next regimes already cannot be described by eqs. (12) because the next unstable mode m = 2 appears. Indeed, taking the experimental values $Re_1 = 1015$, $Re_1' = 1040$ and using (11), we obtain $Re_1^2 = 1115$, which is less than Re = 1140 in the regime g, Fig.6g. At this Reynolds number the dimensionality of effective phase space increases at least from 3 to 5. The above may account for the appearance of additional peak in the spectrum at Re > 1140.

3. EVOLUTION OF ATTRACTOR STRUCTURE

In Section 2 the attractor centered at the unique rapid motion ω_6 was investigated. With a increase in Re the mode ω_2 and the other rapid motions are exited so the question arises about the system behaviour in the effective phase space for this case.

3.1. ω_2-MODE BEHAVIOUR AT N=30

If we compute the ω_2-motion temporal dependence $I_2(t)$ from the experimental data (see the left side of Fig.9), we come to the conclusion that this motion in no way resembles the limiting cycle. On the contrary, this motion occurs by splashes at that moments when the intensity of I_6-motion decreases. This alternation is well traced in the results of regression analysis of I_2-, I_6-modes - see the right side of Fig.9. Here it can be concluded that there exist two domains in the phase space, or two quasiattractors. In the first domain the system moves with frequensies which are adjacent to ω_6 but in the second one it moves with frequensies near ω_2, while the character frequency of travels between these quasiattractors is considerably lower then ω_6 and ω_2. The immediate inspection of the velocity vs. time records shows that this travel frequency increases as Re is increased resulting in additional broadening of the spectral peaks ω_2 and ω_6.

The spectrum in Fig.1b shows that the combinative motions $\omega_6 \pm \omega_2$ appear with the increase in Re. It is natural to suggest these motions to be forced and, due to this fact, not to add new coordinate axes to the effective phase space. To support this suggestion by experiment we carried out a regressive analysis of I_2, I_6 ,

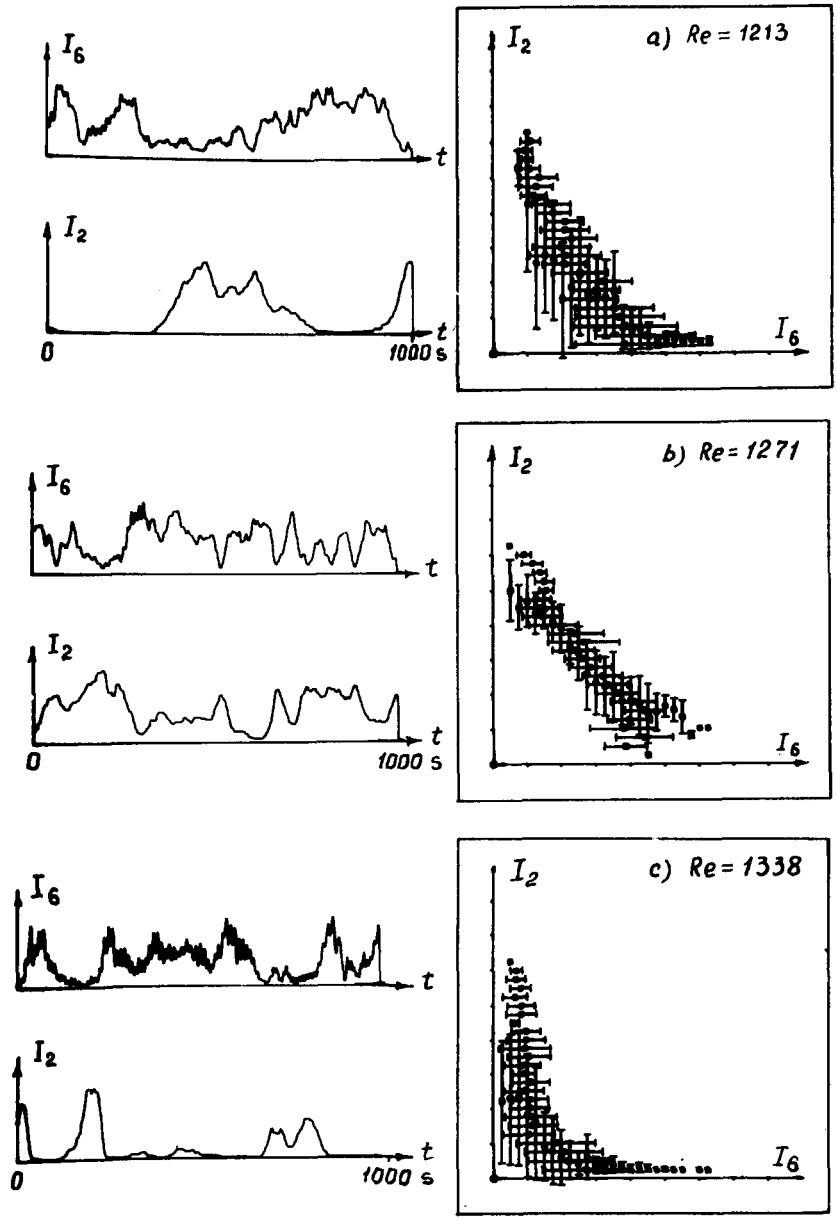

Figure 9. The time dependence of ω_2- and ω_6-motion and the corresponding results of regression analysis of these modes.

and $I_{6\pm2}$ motions - see Fig.10. First of all, the forcing motions I_6 and I_2 are seen to distinctly alternate, this property at smaller Re has already been mentioned. The motions I_{6+2} and I_{6-2} appear to be correlated within the range of small amplitudes only while this correlation practically vanishes at the amplitudes exceeding some average ones. It can be attributed to the fact that at such amplitudes their own non-linear interactions become essential violating the simple relation $I_{6\pm2} \sim I_6 I_2$, which must be fulfilled for forced motions. Indeed, this relation holds relatively good for the mode I_{6-2} (Fig.10c), while the mode I_{6+2} (Fig.10d) reveals greater independence. In conclusion it is possible to say that the combinative mo-

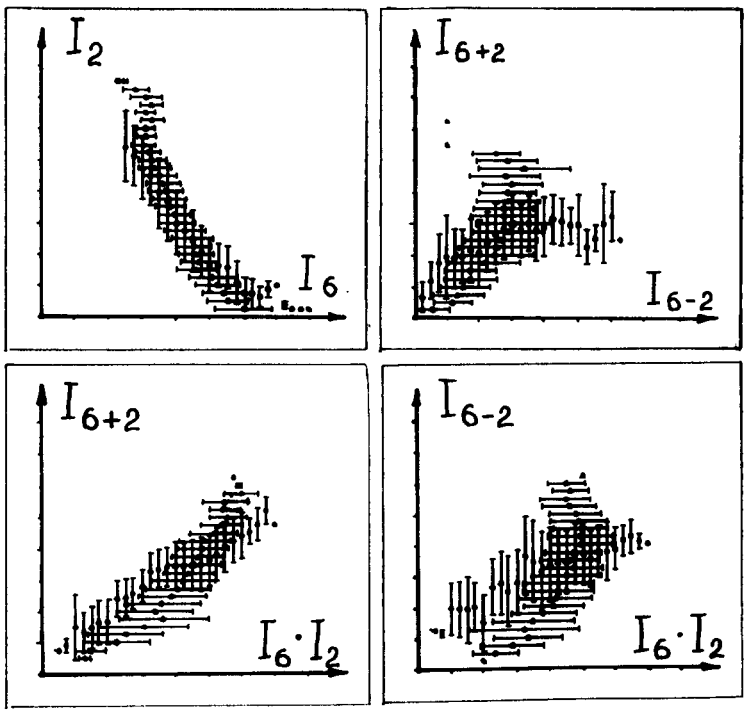

Figure 10. Correlations between the combinative motions $I_{6\pm2}$ and forcing motions I_6, I_2. Re = 1394, N = 30. Frequency window Ω = = 0.05 Hz.

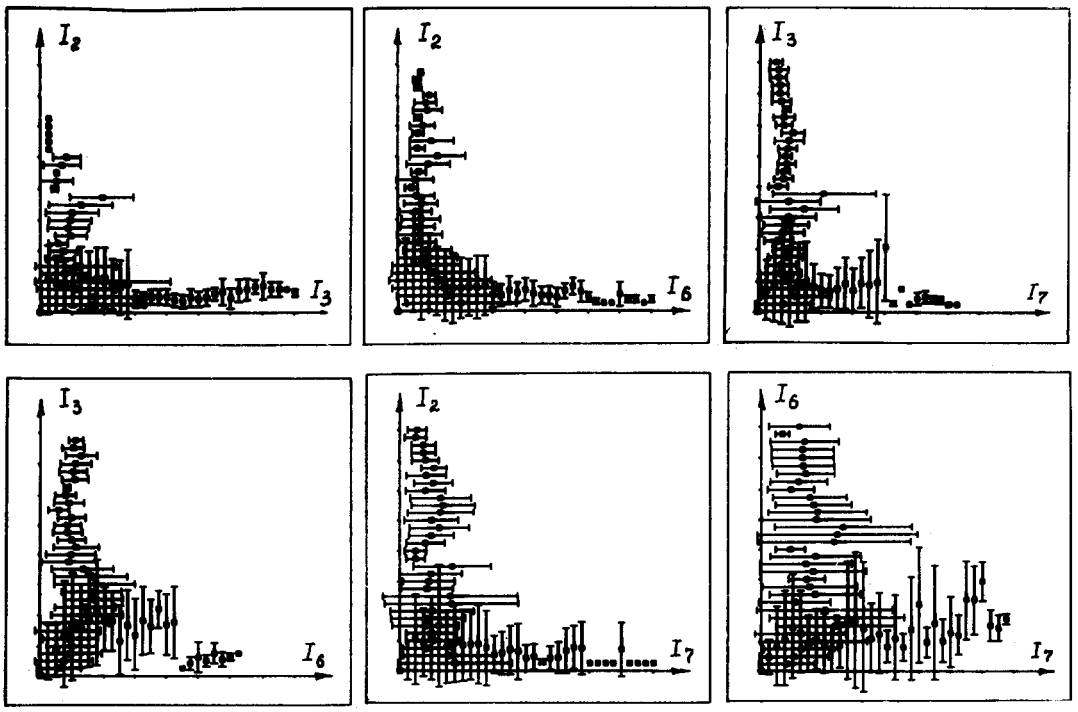

Figure 11. These correlations illustrate a situation when the motion at any one of the frequencies ω_2, ω_3, ω_6, ω_7 excludes the motions at the remaining ones (see the corresponding spectrum in Fig.1c). Frequency window Ω = 0.16 Hz.

tions are forced at small amplitudes only. With an increase in Re and in the presence of random splashes into the region of great amplitudes at fixed Re, the amlitude and phase correlations in the triplets diminish. Hence it is necessary to consider the combinative motions to be the effective degrees of freedom. It is essential that an increase in the number of degrees of freedom occurs not through bifurcations but continuously in this case.

3.2. WANDERING AMONG QUASIATTRACTORS

In the region of high Reynolds numbers the power spectrum contains quite a number of distinctly pronounced peaks of appreciable widths (Fig.1c). Fig.11 shows the results of regression analysis of the motions at frequencies ω_2, ω_3, ω_6 and ω_7 for the velocity record corresponding to the above spectrum. The alternation of the motions ω_2, ω_6 is still clearly traced (Fig.11b). Moreover, this property is an attribute of any pair composed from these four motions. It means that the liquid motion at any one of the four frequencies excludes the motions at the three remaining ones. In other words, the velocity record mainly consists of randomly alternating fragments of sinusoids characterized by the frequencies ω_2, ω_3, ω_6 and ω_7. Comparing this situation with those described above, it is possible to contend that there occurs an increase in the dimensionality of phase space as well as in the number of quasiattractors, between which the phase point wanders. At the same time the frequency of wandering also increases which results in additional broadening of the peaks. When the peak-widths become comparable with the distanses between this peaks, the notion "quasiattractor" loses its sense and the system performs a tangled motion in a high-dimensional phase space.

ACKNOWLEGEMENTS

The authors would like to express their acknowlegements to Yu.E.Nesterikhin for his permanent attention and support, to E.A.Kuznetsov and M.D.Spector for valuable discussions and helpful suggestions. The authors are also grateful to Z.B.Krugljak, V.S.Sobolev and E.N.Utkin for the special device development and help during the course of experiment. As well we are indebted to F.A.Zhuravel who developed the acquisition software.

REFERENCES:

[1] Lubimov, D.V., Putin, G.F., Chernatinsky, V.I., Dokl. Akad. Nauk SSSR, 235 (1977) 554-556.
[2] Rabinovitch, M.I., Uspehi Fiz. Nauk 125 (1978) 123-168.
[3] McLaughlin, J.B. and Martin, P.C., Phys. Rev. A12 (1975) 186-203.
[4] Lorenz, E.N., J.Atmos.Sci. 20 (1963) 130-141.
[5] Arnold, V.I., in: Nelineinie volni (Nauka, Moscow, 1979).
[6] Landau, L.D. and Lifshits, E.M., Mekhanika sploshn. sred (Gostekhizdat, Moscow, 1953).
[7] Kuznetsov, E.A., et al., Preprint No.58 (Inst. of Autom. and Electrometry, Novosibirsk, 1977).
[8] Zhuravel, F.A. et al., Preprint No.103 (Inst. of Autom. and Electrometry, Novosibirsk, 1979).
[9] Fenstermacher, P.R., Swinney, H.L., Gollub, J.P., J.Fluid Mech. 94 (1979) 103-128.
[10] Walden, R.W. and Donnelly, R.J., Phys. Rev. Lett. 42 (1979) 301-304.
[11] L'vov, V.S. and Predtechensky, A.A., Preprint No.111 (Inst. of Autom. and Electrometry, Novosibirsk, 1979).
[12] Kuznetsov, E.A., L'vov, V.S., Predtechensky, A.A et al., Pisma Zh. Eksp. Teor. Fiz. 30 (1979) 226-229.
[13] Rabinovitch, M.I. and Fabricant, A.L., Zh.Eksp.Teor.Fiz. 77 (1979) 617-629.